

# <sup>1</sup> SenAOReFoc: A Closed-Loop Sensorbased Adaptive Optics and Remote Focusing Control Software

<sup>3</sup> **Jiahe Cui<sup>\*1</sup>, Karen M. Hampson<sup>1</sup>, Matthew Wincott<sup>1</sup>, and Martin J. Booth<sup>1</sup>**

<sup>5</sup> **1 Department of Engineering Science, University of Oxford, Parks Road, Oxford, OX1 3PJ, UK**

DOI: [10.xxxxxx/draft](https://doi.org/10.xxxxxx/draft)

## Software

- [Review ↗](#)
- [Repository ↗](#)
- [Archive ↗](#)

---

**Editor:** [Patrick Diehl](#) ↗

**Reviewers:**

- [@abhilash12iec002](#)
- [@jacktyson](#)
- [@alvesjnr](#)

**Submitted:** 21 December 2021

**Published:** unpublished

## License

Authors of papers retain  
copyright and release the work  
under a Creative Commons  
Attribution 4.0 International  
License ([CC BY 4.0](#)).

## <sup>6</sup> Summary

<sup>7</sup> SenAOReFoc is a closed-loop sensorbased adaptive optics (AO) and remote focusing control  
<sup>8</sup> software that works with a deformable mirror (DM) and a Shack-Hartmann wavefront sensor  
<sup>9</sup> (SHWS). It provides a user-friendly graphic user interface (GUI) with modular widget arrange-  
<sup>10</sup> ments and clear labelling to help the user navigate through different software functionalities.  
<sup>11</sup> Interactive messages are also displayed from the GUI for user guidance.

<sup>12</sup> SenAOReFoc consists of 5 main units, the SHWS initialisation and DM calibration unit, the  
<sup>13</sup> Zernike aberration input unit, the AO control and data collection unit, the miscellaneous control  
<sup>14</sup> unit, and the remote focusing unit, as shown in [Figure 1](#). The software can be ran in either  
<sup>15</sup> 'debug mode' to perform functionality tests without connected hardware (DM and SHWS),  
or 'standard mode' on a well-aligned optical sectioning microscope (confocal, multiphoton,  
etc.). User controllable system parameters can be freely accessed and modified in a separate  
configuration file that is loaded upon software initialisation, and parameters that require  
continuous user input can be modified from the GUI. Parameters calculated when running  
the software, as well as important result data, are grouped and saved in a separate HDF5  
file that can be read with HDFView software. Automated AO performance characterisations  
can be performed in 'standard mode' to assess the correction ability of the optical system. If  
the adopted DM is designed with a large stroke, i.e., is capable of large deformations, both  
the closed-loop AO correction and remote focusing functionalities can be exploited. On the  
other hand, if the DM exhibits insufficient stroke for remote focusing, by ignoring the remote  
focusing unit, closed-loop AO correction functionalities will still be fully functional without  
additional modifications to the software.

<sup>28</sup> Closed-loop AO correction can be performed using both the zonal method, which updates  
<sup>29</sup> DM control voltages in terms of the raw slope values; and the modal method, which updates  
<sup>30</sup> DM control voltages in terms of orthogonal Zernike polynomials. There are four sub-modes  
<sup>31</sup> tagged to each of the two methods: 1) standard closed-loop AO correction; 2) closed-loop AO  
<sup>32</sup> correction with consideration of obscured search blocks; 3) closed-loop AO correction with  
<sup>33</sup> partial correction excluding defocus; and 4) closed-loop AO correction with both considera-  
<sup>34</sup> tion of obscured search blocks and partial correction excluding defocus.

<sup>35</sup> Remote focusing can be performed by scanning the focus axially with a pre-determined axial  
<sup>36</sup> range, step increment and step number, or by manually adjusting a toggle bar on the GUI for  
<sup>37</sup> random access remote focusing. The former also incorporates options of whether or not to  
<sup>38</sup> perform closed-loop AO correction at each remote focusing depth.

---

\*[jiahe.cui@eng.ox.ac.uk](mailto:jiahe.cui@eng.ox.ac.uk)

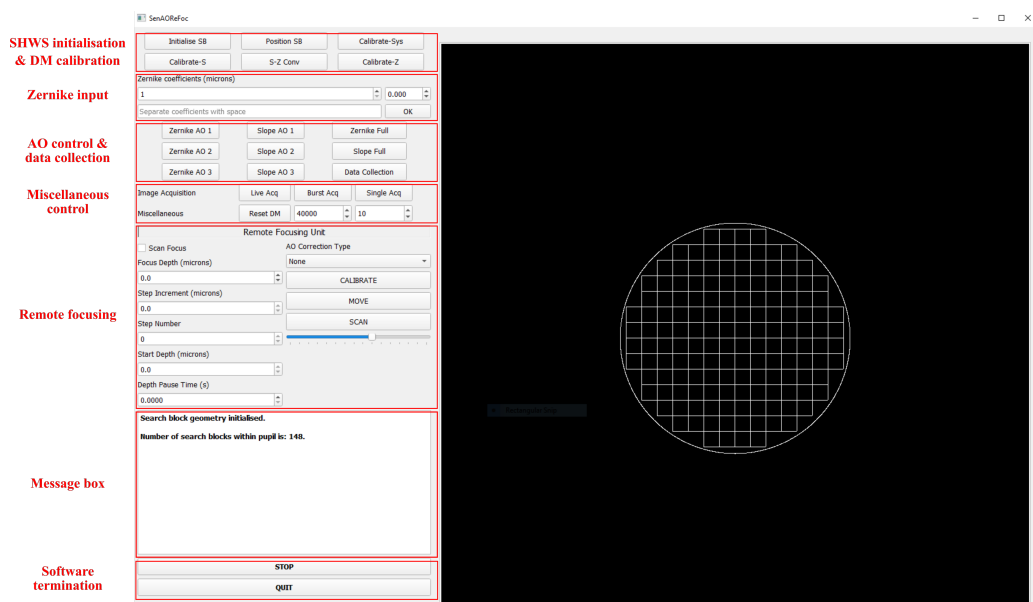


**Figure 1:** Graphic user interface (GUI) of SenAOReFoc with modular units labelled in red boxes.

## 39 Statement of need

40 The performance of optical microscopes degrades significantly in the presence of optical  
41 aberrations that develop due to misalignments in the optical system and inhomogeneities in  
42 refractive index of the imaging sample. This results in compromised image resolution and  
43 contrast. Adaptive optics (AO) is a powerful technique that corrects for optical aberrations  
44 using reconfigurable adaptive devices, such as a deformable mirror (DM) or spatial light  
45 modulator (SLM), to restore the image quality (Booth, 2014). This is most crucial for  
46 high-quality imaging, such as super-resolution or deep imaging.

47 Remote focusing is an axial scanning technique recently introduced to avoid slow movements  
48 of the sample stage and objective lens during real-time applications (Ji et al., 2016). By using  
49 a DM for remote focusing, calibration can be performed through closed-loop AO correction  
50 to simultaneously correct for system aberrations introduced by beam divergence at different  
51 focusing depths (Žurauskas et al., 2017).

52 Sensorbased AO, which uses a dedicated sensor to measure the wavefront (Platt & Shack,  
53 2001), was first introduced in the field of astronomy (Beckers, 1993). Since then, it has also  
54 been widely adopted in vision science (Godara et al., 2010; Porter et al., 2006) and microscopy  
55 (Booth, 2007; Ji, 2017). A range of software serving for different astronomical purposes have  
56 been introduced over time, including those for simulation of AO systems (Carbilliet et al., 2005;  
57 Conan & Correia, 2014), control with atmospheric tomography (Ahmadia & Ellerbroek, 2005),  
58 and fast control using GPU hardware (Guyon et al., 2018). In the microscopy community,  
59 software is also openly available for AO modelling and analysis (Townson et al., 2019), as well  
60 as general AO control (Hall et al., 2020). However, there is not yet an existing open-source  
61 software that serves the purpose of performing both AO and remote focusing within the single  
62 package, despite that the techniques have been widely adopted. As a result, time and effort  
63 has to be spent reimplementing existing techniques for different hardware systems.

64 SenAOReFoc aims to fill this gap and to make closed-loop sensorbased AO (Fernández et al.,  
65 2001) and remote focusing more easily accessible to the microscopy community. It has been  
66 designed for open development and easy integration into existing adaptive optical microscopes  
67 with a simple and user-friendly architecture. The functionality of the software has also been  
68 tested on different operating systems (Windows/Linux/macOS) for sake of generality. The

69 software fully operates in Windows under both ‘debug mode’ and ‘standard mode’ for hardware  
70 control. For Linux and macOS, functionality tests in ‘debug mode’ passes for both systems  
71 when hardware packages are not imported. Python-bindings for Ximea cameras and Python  
72 3.8-binding for Alpaq DMs are compatible with Linux systems, and other Python-bindings for  
73 Alpaq DMs in Linux should also be compatible following their release. However, we note that  
74 SenAOReFoc is a control software, and the performance of the closed-loop AO correction in  
75 practice is inevitably dependent on the state of the optical system. Finally, SenAOReFoc takes  
76 care of some reported issues in the field, such as the thermal effects of electromagnetic DMs  
77 ([Bitenc, 2017](#)), and obscured search blocks in the case of severely distorted pupils ([Cui et al., 2020](#);  
78 [Dong & Booth, 2018](#); [Ye et al., 2015](#)). In the former case, an option is provided to  
79 exercise the DM membrane by sending routine sets of random control voltages to the actuators  
80 upon software initialisation. In the latter case, control algorithms for both the zonal and modal  
81 methods are modified as compared to the standard case to ensure the orthogonality of control.

## 82 Example usage

83 Four examples are given for the usage of this software, the first three for automated AO  
84 performance characterisations of the reflectance confocal microscope described in ([Cui, Turcotte,  
85 Hampson, et al., 2021](#); [Cui, Turcotte, Emptage, et al., 2021](#)); and the last for remote focusing  
86 in frozen mouse skull as reported in ([Cui, Turcotte, Hampson, et al., 2021](#)).

87 **Example 1:** The dynamic range of the SHWS for the first  $N$  Zernike modes can be characterised  
88 by generating and correcting for them in closed-loop using mode 0/1 of [Data Collection].  
89 [Figure 2\(a\)](#) provides an example when characterising Zernike modes 3-20 (excl. tip/tilt).  
90 [Figure 2\(b\)-\(e\)](#) provide examples of generated and detected RMS amplitudes of selected  
91 odd/even Zernike modes in increments of 0.02 micrometers. Parameters in config.yaml under  
92 AO and data\_collect were set as follows.

```
A0:  
control_coeff_num: 20 # Number of zernike modes to control during AO correction  
  
data_collect:  
    data_collect_mode: 1 # Mode flag for Data Collection button, detailed function descri  
    loop_max_gen: 15 # Maximum number of loops during closed-loop generation of zernike m  
    incre_num: 15 # Number of zernike mode amplitudes to generate in mode 0/1  
    incre_amp: 0.02 # Increment amplitude between zernike modes in mode 0/1  
    run_num: 5 # Number of times to run mode 0/1/2/3
```

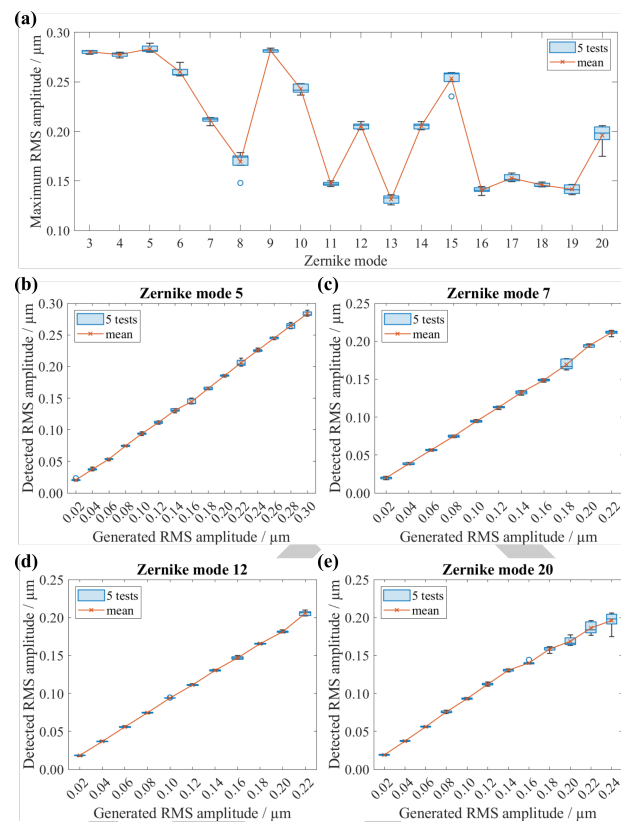


**Figure 2:** Characterisation results of system AO correction performance. (a) Dynamic range of the SHWS for Zernike modes 3-20 (excl. tip/tilt). (b)-(e) Generated and detected RMS amplitudes of odd/even Zernike modes (b) 5, (c) 7, (d) 12, and (e) 20, in increments of 0.02 micrometers. 5 tests were performed for each measurement.

93     **Example 2:** The degree of Zernike mode coupling upon detection at the SHWS can be  
94     characterised by individually generating the same amount of each mode on the DM and  
95     constructing a heatmap of the detected Zernike coefficients using mode 0/1 of [Data Collection].  
96     Figure 3 provides an example heatmap of correlation coefficients between detected and  
97     generated mode values for 0.1 micrometers of Zernike modes 3-20 (excl. tip/tilt). Parameters  
98     in config.yaml under data\_collect were set as follows.

```
data_collect:
  data_collect_mode: 1 # Mode flag for Data Collection button, detailed function descri
  loop_max_gen: 15 # Maximum number of loops during closed-loop generation of zernike m
  incre_num: 1 # Number of zernike mode amplitudes to generate in mode 0/1
  incre_amp: 0.1 # Increment amplitude between zernike modes in mode 0/1
  run_num: 5 # Number of times to run mode 0/1/2/3
```

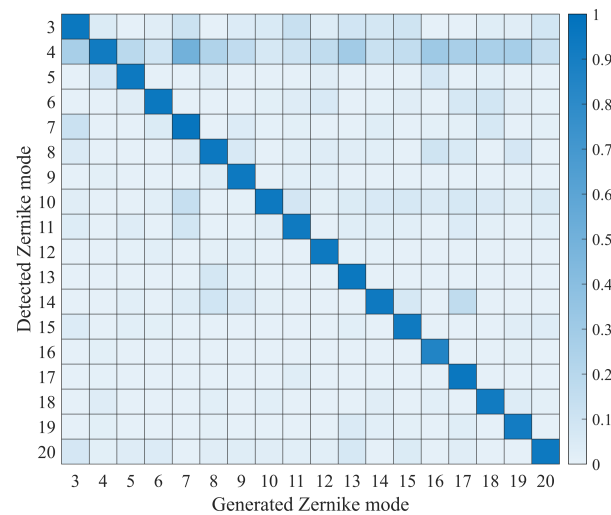


**Figure 3:** Heatmap of correlation coefficients between detected and generated mode values for 0.1 micrometers of Zernike modes 3-20 (excl. tip/tilt).

99   **Example 3:** To ensure the system can correct for multiple Zernike modes with good stability  
100 and minimal mode coupling, different combinations of odd and even Zernike modes can be be  
101 generated and corrected for in closed-loop using mode 2/3 of [Data Collection]. **Figure 4**  
102 provides an example of the detect amplitude and Strehl ratio after each closed-loop iteration  
103 for some odd and even Zernike mode combinations. Parameters in config.yaml under  
104 data\_collect were set as follows.

```
data_collect:  

  data_collect_mode: 3 # Mode flag for Data Collection button, detailed function descri...  

  loop_max_gen: 15 # Maximum number of loops during closed-loop generation of zernike ...  

  run_num: 5 # Number of times to run mode 0/1/2/3
```

105 And [Zernike array edit box] was set to [0 0 0 0 **0.1** 0 **0.1** 0 0 0 0 **0.1** 0 0 0 0 0 0 **0.1**].

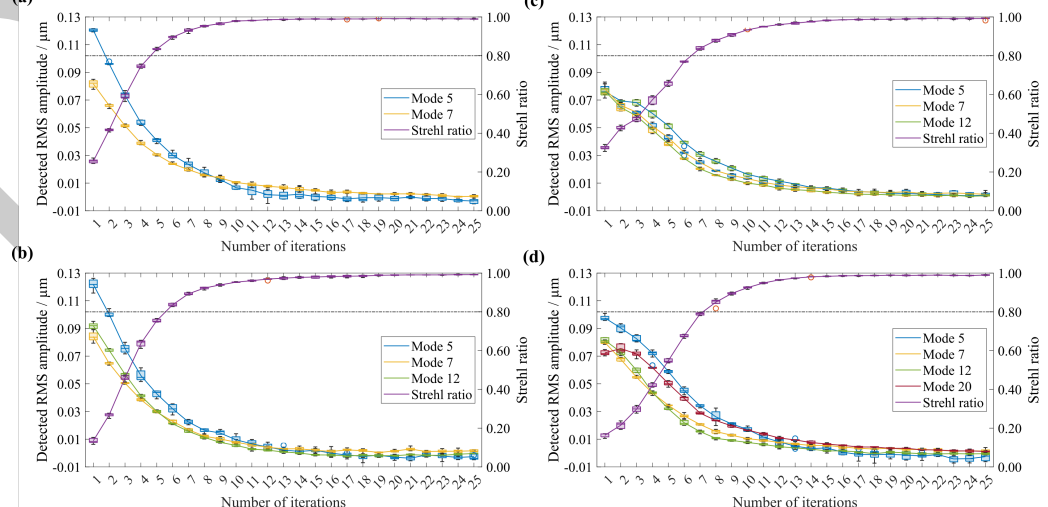


**Figure 4:** Detected amplitudes of generated odd and even Zernike mode combinations and Strehl ratio calculated using first 69 Zernike modes (excl. tip/tilt) after each closed-loop iteration. 5 tests were performed for each measurement.

106   **Example 4:** Voltages that control DM actuators to deform the membrane for fine axial  
 107   remote focusing was calibrated according to the procedure explained in the GitHub repository  
 108   <https://github.com/jiahecui/SenAOReFoc>, and reported in (Cui, Turcotte, Hampson, et al.,  
 109   2021) and (Cui, Turcotte, Emptage, et al., 2021). [Calibrate] was pressed for both directions  
 110   of the optical axis and a piece of white card was displaced by 10 micrometers each time  
 111   before pressing 'y' on the keyboard to proceed with closed-loop AO correction. Interpolation  
 112   of the DM control voltages at each calibration step was then performed to obtain those for  
 113   0.1 micrometer increments. The software's remote focusing capability was demonstrated in  
 114   frozen mouse skull in (Cui, Turcotte, Hampson, et al., 2021) to show no noticeable difference  
 115   in resolution and size of field of view as compared to standard translation of the sample stage.  
 116   Results are also shown in Figure 5.

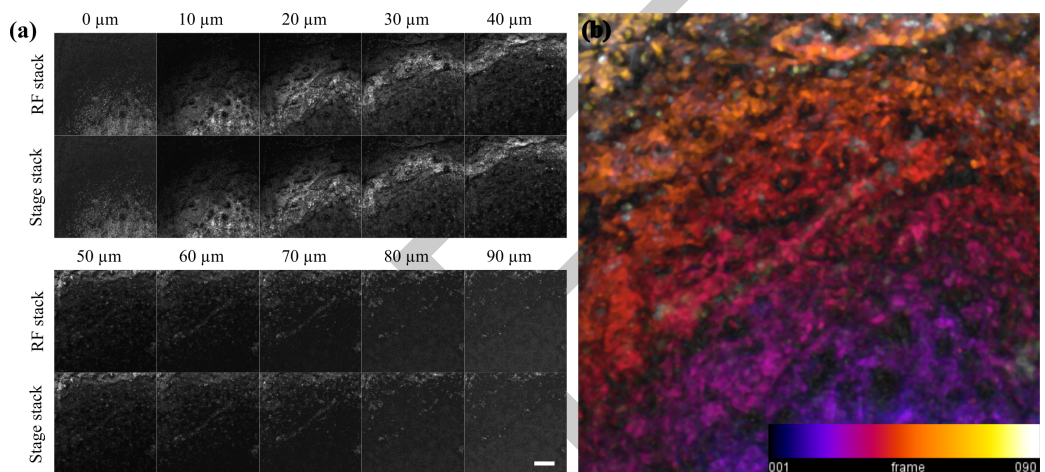


**Figure 5:** Remote focusing results within frozen mouse skull. (a) Stack images acquired with 10 micrometer axial steps over a 90 micrometer depth range. Top rows: results obtained by scanning sequentially through multiple depths using precalibrated DM control voltages. Bottom rows: comparison results obtained by axially translating the sample stage only. (b) Colour-coded maximum intensity projection of 90 frames with 1 micrometer intervals. Scale bar: 100 micrometers.

## 117 How to cite

118   If you're using any modified version of this software for your work, please cite this paper. If  
 119   you're performing remote focusing using the calibration procedure set out in this software,  
 120   please also cite either (Cui, Turcotte, Hampson, et al., 2021) or (Cui, Turcotte, Emptage, et  
 121   al., 2021).

## 122 Acknowledgements

123   We thank Chao He for testing the software functionality using different operating systems.  
 124   This work was supported by European Research Council projects 695140 and 812998.

## 125 References

- 126   Ahmadia, A., & Ellerbroek, B. (2005). A software framework for fast adaptive optics con-  
 127   trol with atmospheric tomography [Conference Proceedings]. *Adaptive Optics: Analysis*  
 128   *and Methods/Computational Optical Sensing and Imaging/Information Photonics/Signal*  
 129   *Recovery and Synthesis Topical Meetings on CD-ROM*, ATbB4. <https://doi.org/10.1364/AOPT.2005.ATHB4>

- 131 Beckers, J. M. (1993). Adaptive optics for astronomy: Principles, performance, and applications  
132 [Journal Article]. *Annual Review of Astronomy and Astrophysics*, 31(1), 13–62. <https://doi.org/10.1146/annurev.aa.31.090193.000305>
- 134 Bitenc, U. (2017). Software compensation method for achieving high stability of alpao  
135 deformable mirrors. *Optics Express*, 25(4), 4368–4381. <https://doi.org/10.1364/OE.25.004368>
- 137 Booth, M. J. (2007). Adaptive optics in microscopy [Journal Article]. *Philosophical Transactions of the Royal Society A: Mathematical, Physical and Engineering Sciences*, 365(1861),  
138 2829–2843. <https://doi.org/10.1098/rsta.2007.0013>
- 140 Booth, M. J. (2014). Adaptive optical microscopy: The ongoing quest for a perfect image.  
141 *Light: Science & Applications*, 3, e165. <https://doi.org/10.1038/lsci.2014.46>
- 142 Carbillot, M., Véronaud, C., Femenía, B., Riccardi, A., & Fini, L. (2005). Modelling astronomical  
143 adaptive optics - i. The software package caos [Journal Article]. *Monthly Notices of the  
144 Royal Astronomical Society*, 356(4), 1263–1275. <https://doi.org/10.1111/j.1365-2966.2004.08524.x>
- 146 Conan, R., & Correia, C. (2014). Object-oriented matlab adaptive optics toolbox [Conference  
147 Proceedings]. *SPIE Astronomical Telescopes + Instrumentation*, 9148. <https://doi.org/10.1111/12.2054470>
- 149 Cui, J., Dong, B., & Booth, M. J. (2020). *Shack-hartmann sensing with arbitrarily shaped  
150 pupil*. <https://doi.org/10.5281/zenodo.3885508>
- 151 Cui, J., Turcotte, R., Emptage, N. J., & Booth, M. J. (2021). Extended range and aberration-  
152 free autofocusing via remote focusing and sequence-dependent learning [Journal Article].  
153 *Optics Express*, 29(22), 36660–36674. <https://doi.org/10.1364/OE.442025>
- 154 Cui, J., Turcotte, R., Hampson, K., Emptage, N. J., & Booth, M. J. (2021). Remote-  
155 focussing for volumetric imaging in a contactless and label-free neurosurgical microscope.  
156 *Biophotonics Congress 2021*, DTh2A.2. <https://doi.org/10.1364/boda.2021.dth2a.2>
- 157 Dong, B., & Booth, M. J. (2018). Wavefront control in adaptive microscopy using shack-  
158 hartmann sensors with arbitrarily shaped pupils. *Optics Express*, 26(2), 1655–1669. <https://doi.org/10.1364/OE.26.001655>
- 160 Fernández, E. J., Iglesias, I., & Artal, P. (2001). Closed-loop adaptive optics in the human eye  
161 [Journal Article]. *Optics Letters*, 26(10), 746–748. <https://doi.org/10.1364/OL.26.000746>
- 162 Godara, P., Dubis, A. M., Roorda, A., Duncan, J. L., & Carroll, J. (2010). Adaptive optics  
163 retinal imaging: Emerging clinical applications [Journal Article]. *Optometry and Vision  
164 Science : Official Publication of the American Academy of Optometry*, 87(12), 930–941.  
165 <https://doi.org/10.1097/OPX.0b013e3181ff9a8b>
- 166 Guyon, O., Sevin, A., Gratadour, D., Bernard, J., Ltaief, H., Sukkari, D., Cetre, S., Skaf, N.,  
167 Lozi, J., Martinache, F., Clergeon, C., Norris, B., Wong, A., & Males, J. (2018). The  
168 compute and control for adaptive optics (CACAO) real-time control software package  
169 [Book]. *SPIE Astronomical Telescopes + Instrumentation*, 10703. <https://doi.org/10.1111/12.2314315>
- 171 Hall, N., Titlow, J., Booth, M. J., & Dobbie, I. M. (2020). Microscope-AOtools: A generalised  
172 adaptive optics implementation. *Optics Express*, 28(20), 28987–29003. <https://doi.org/10.1364/OE.401117>
- 174 Ji, N. (2017). Adaptive optical fluorescence microscopy [Journal Article]. *Nature Methods*, 14,  
175 374. <https://doi.org/10.1038/nmeth.4218>
- 176 Ji, N., Freeman, J., & Smith, S. L. (2016). Technologies for imaging neural activity in large  
177 volumes. *Nature Neuroscience*, 19, 1154. <https://doi.org/10.1038/nn.4358>

- 178 Platt, B. C., & Shack, R. (2001). History and principles of shack-hartmann wavefront sensing  
179 [Journal Article]. *Journal of Refractive Surgery*, 17(5), S573–S577. <https://doi.org/10.3928/1081-597X-20010901-13>
- 181 Porter, J., Queener, H., Lin, J., Thorn, K., & Awwal, A. A. (2006). *Adaptive optics for vision*  
182 *science: Principles, practices, design, and applications* (Vol. 171). John Wiley & Sons.
- 183 Townson, M. J., Farley, O. J. D., Orban de Xivry, G., Osborn, J., & Reeves, A. P. (2019).  
184 AOtools: A python package for adaptive optics modelling and analysis. *Optics Express*,  
185 27(22), 31316–31329. <https://doi.org/10.1364/OE.27.031316>
- 186 Ye, J., Wang, W., Gao, Z., Liu, Z., Wang, S., Benítez, P., Miñano, J. C., & Yuan, Q.  
187 (2015). Modal wavefront estimation from its slopes by numerical orthogonal transformation  
188 method over general shaped aperture. *Optics Express*, 23(20), 26208–26220. <https://doi.org/10.1364/OE.23.026208>
- 190 Žurauskas, M., Barnstedt, O., Frade-Rodriguez, M., Waddell, S., & Booth, M. J. (2017).  
191 Rapid adaptive remote focusing microscope for sensing of volumetric neural activity [Journal  
192 Article]. *Biomedical Optics Express*, 8(10), 4369–4379. <https://doi.org/10.1364/BOE.8.004369>